Radiosynthesis and Evaluation of ^{11}C-CIMBI-5 as a 5-HT$_{2A}$ Receptor Agonist Radioligand for PET

Anders Ettrup[1], Mikael Palner[1], Nic Gillings[2], Martin A. Santini[1], Martin Hansen[3], Birgitte R. Kornum[1], Lars K. Rasmussen[3], Kjell Någren[2], Jacob Madsen[2], Mikael Begtrup[3], and Gitte M. Knudsen[1]

[1]Neurobiology Research Unit and Center for Integrated Molecular Brain Imaging (CIMBI), Copenhagen University Hospital, Rigshospitalet, Copenhagen, Denmark; [2]PET and Cyclotron Unit, Copenhagen University Hospital, Rigshospitalet, Copenhagen, Denmark; and [3]Department of Medicinal Chemistry, Faculty of Pharmaceutical Sciences, University of Copenhagen, Copenhagen, Denmark

PET brain imaging of the serotonin 2A (5-hydroxytryptamine 2A, or 5-HT$_{2A}$) receptor has been widely used in clinical studies, and currently, several well-validated radiolabeled antagonist tracers are used for in vivo imaging of the cerebral 5-HT$_{2A}$ receptor. Access to 5-HT$_{2A}$ receptor agonist PET tracers would, however, enable imaging of the active, high-affinity state of receptors, which may provide a more meaningful assessment of membrane-bound receptors. In this study, we radiolabel the high-affinity 5-HT$_{2A}$ receptor agonist 2-(4-iodo-2,5-dimethoxyphenyl)-*N*-(2-[^{11}C-OCH$_3$]methoxybenzyl)ethanamine (^{11}C-CIMBI-5) and investigate its potential as a PET tracer. **Methods:** The in vitro binding and activation at 5-HT$_{2A}$ receptors by CIMBI-5 was measured with binding and phosphoinositide hydrolysis assays. Ex vivo brain distribution of ^{11}C-CIMBI-5 was investigated in rats, and PET with ^{11}C-CIMBI-5 was conducted in pigs. **Results:** In vitro assays showed that CIMBI-5 was a high-affinity agonist at the 5-HT$_{2A}$ receptor. After intravenous injections of ^{11}C-CIMBI-5, ex vivo rat studies showed a specific binding ratio of 0.77 ± 0.07 in the frontal cortex, which was reduced to cerebellar levels after ketanserin treatment, thus indicating that ^{11}C-CIMBI-5 binds selectively to the 5-HT$_{2A}$ receptor in the rat brain. The PET studies showed that the binding pattern of ^{11}C-CIMBI-5 in the pig brain was in accordance with the expected 5-HT$_{2A}$ receptor distribution. ^{11}C-CIMBI-5 gave rise to a cortical binding potential of 0.46 ± 0.12, and the target-to-background ratio was similar to that of the widely used 5-HT$_{2A}$ receptor antagonist PET tracer ^{18}F-altanserin. Ketanserin treatment reduced the cortical binding potentials to cerebellar levels, indicating that in vivo ^{11}C-CIMBI-5 binds selectively to the 5-HT$_{2A}$ receptor in the pig brain. **Conclusion:** ^{11}C-CIMBI-5 showed a cortex-to-cerebellum binding ratio equal to the widely used 5-HT$_{2A}$ antagonist PET tracer ^{18}F-altanserin, indicating that ^{11}C-CIMBI-5 has a sufficient target-to-background ratio for future clinical use and is displaceable by ketanserin in both rats and pigs. Thus, ^{11}C-CIMBI-5 is a promising tool for investigation of 5-HT$_{2A}$ agonist binding in the living human brain.

Key Words: PET tracer development; agonist; porcine; serotonin receptors

J Nucl Med 2010; 51:1763–1770
DOI: 10.2967/jnumed.109.074021

Serotonin 2A (5-hydroxytryptamine 2A, or 5-HT$_{2A}$) receptors are implicated in the pathophysiology of human diseases such as depression, Alzheimer's disease, and schizophrenia. Also, 5-HT$_{2A}$ receptor stimulation exerts the hallucinogenic effects of recreational drugs such as lysergic acid diethylamide and 1-(2,5-dimethoxy-4-iodophenyl)-2-aminopropane (*1*), and atypical antipsychotics have antagonistic or inverse agonistic effects on the 5-HT$_{2A}$ receptor (*2*).

Currently, there are 3 selective 5-HT$_{2A}$ antagonistic PET ligands—^{18}F-altanserin (*3*), ^{18}F-deuteroaltanserin (*4*), and ^{11}C-MDL100907 (*5*)—in use for mapping and quantifying 5-HT$_{2A}$ receptor binding in the human brain. However, whereas 5-HT$_{2A}$ antagonists bind to the total pool of receptors, 5-HT$_{2A}$ agonists bind only to the high-affinity state of the receptor (*6,7*). Thus, a 5-HT$_{2A}$ receptor agonist ligand holds promise for the selective mapping of 5-HT$_{2A}$ receptors in their functional state; therefore, alterations in agonist binding measured in vivo with PET may be more relevant for assessing dysfunction in the 5-HT$_{2A}$ receptor system in specific patient or population groups. Furthermore, because many of the 5-HT$_{2A}$ receptors are intracellularly localized (*8,9*), combining measurements with antagonist and agonist PET tracers would enable determination of the ratio of the high-affinity, membrane-bound, and active receptors to the low-affinity, intracellular, and inactive receptors (*10*). Thus, quantification of functionally active 5-HT$_{2A}$ receptors in vivo using an agonist PET tracer is hypothesized to be superior to antagonist measurements of total number of 5-HT$_{2A}$ receptors for studying alterations in receptor function in human diseases such as depression.

D$_2$ receptor agonist radiotracers are now known to be superior to antagonist radiotracers in measuring dopamine release in vivo in monkeys (*11*) and mice (*10*). In humans,

Received Jan. 26, 2010; revision accepted Aug. 11, 2010.
For correspondence or reprints contact: Anders Ettrup, Neurobiology Research Unit, Blegdamsvej 9, Rigshospitalet, Bldg. 9201, DK-2100 Copenhagen, Denmark.
E-mail: ettrup@nru.dk

most studies have found that 5-HT_{2A} receptor antagonist PET tracers are not displaceable by elevated levels of endogenous serotonin (5-HT) (*12*). This suggests that agonist PET tracers may be better suited for measuring endogenous competition than antagonist tracers, so that 5-HT_{2A} receptor agonists would be more prone to displacement by competition with endogenously released 5-HT. Monitoring the release of endogenous 5-HT is highly relevant in relation to human diseases such as depression and Alzheimer's disease, which involve dysfunction of the 5-HT system.

2-(4-iodo-2,5-dimethoxyphenyl)-*N*-(2-methoxybenzyl) ethanamine (25I-NBOMe, or CIMBI [Center for Integrated Molecular Brain Imaging]-5) has recently been described as a potent and selective 5-HT_{2A} receptor agonist, and phosphoinositide hydrolysis assays revealed that it has a 12-fold lower half-maximal effective concentration (EC_{50}) than 5-HT itself (*13*). Although this compound has been tritiated (*14*), its in vivo biological distribution and possible PET tracer potential have not been investigated.

Here, we present the synthesis of ^{11}C-labeled CIMBI-5 and biological evaluation of this novel PET tracer. The compound was characterized in vitro, and ^{11}C-CIMBI-5 was investigated after intravenous injection both ex vivo in rats and in vivo in pigs with PET.

MATERIALS AND METHODS

In Vitro Binding and Activation

Inhibition constant (K_i) determinations against various neuroreceptors (Table 1) were provided by the Psychoactive Drug Screening Program (PDSP; experimental details are provided at http://pdsp.med.unc.edu/). In our laboratory, competition binding experiments were performed on a NIH-3T3 cell line (GF62) stably transfected with the rat 5-HT_{2A} receptor as previously described (*15*) using 0.2 nM ^{3}H-MDL100907 (kindly provided by Prof. Christer Halldin) and 8 different concentrations of CIMBI-5 (1 μM to 1 pM) in a total of 1 mL of buffer (500 mM Tris base, 1,500 mM NaCl, and 200 mM ethylenediaminetetraacetic acid). Nonspecific binding was determined with 1 μM ketanserin. Incubation was performed for 1 h at 37°C.

TABLE 1
PDSP Screening Result: Inhibition Constants (K_i) for CIMBI-5 Versus Serotonin and Other Receptors

Receptor	K_i (nM)
5-HT_{2A}	2.2 ± 0.1
5-HT_{2B}	2.3 ± 0.2
5-HT_{2C}	7.0 ± 1.0
5-HT_6	58 ± 17
5-HT_{1A}	85 ± 16
D_3	117 ± 14
α_{2C}	348 ± 17
D_4	647 ± 37
Serotonin transporter	1,009 ± 84
α_{2A}	1,106 ± 206
M_5	1,381 ± 231
D_2	1,600 ± 333
5-HT_7	1,670 ± 125
5-HT_{5A}	2,200 ± 385
D_1	3,718 ± 365
5-HT_{1B}	3,742 ± 553
Norepinephrine transporter	4,574 ± 270
Dopamine transporter	5,031 ± 343
D_5	7,872 ± 933

The 5-HT_{2A} receptor activation by CIMBI-5 was measured on GF62 cells using a phosphoinositide hydrolysis assay as previously described (*16*). Briefly, cells were incubated with myo-(*1,2*)-^{3}H-inositol (Amersham) in labeling medium. Subsequently, the cells were washed and incubated at 37°C with CIMBI-5 (1 μM to 0.1 pM). The formed inositol phosphates were extracted and counted with a liquid scintillation counter.

Radiochemical Synthesis of ^{11}C-CIMBI-5

^{11}C-methyl trifluoromethanesulfonate (triflate) produced using a fully automated system was transferred in a stream of helium to a 1.1-mL vial containing 0.3–0.4 mg of the labeling precursor (**3**; Fig. 1) and 2 μL of 2 M NaOH in 300 μL of acetonitrile, and the resulting mixture was heated at 40°C for 30 s. Subsequently, 250 μL of trifluoroacetic acid:CH_3CN (1:1) were added and the mixture heated at 80°C for 5 min (Fig. 2). After neutralization with 750 μL of 2 M NaOH, the reaction mixture was purified by high-performance liquid chromatography (HPLC) on a Luna C18 column (Phenomenex Inc.) (250 × 10 mm; 40:60 acetonitrile:25 mM citrate buffer, pH 4.7; and flow rate, 5 mL/min). The chemical synthesis of the labeling precursor is described in detail in the supplemental data (supplemental materials are available online only at http://jnm.snmjournals.org).

The fraction corresponding to the labeled product (~12.5 min) was collected in 50 mL of 0.1% ascorbic acid, and the resulting solution was passed through a solid-phase C18 Sep-Pak extraction column (Waters Corp.), which had been preconditioned with 10 mL of ethanol, followed by 20 mL of 0.1% ascorbic acid. The column was flushed with 3 mL of sterile water. Then, the trapped radioactivity was eluted with 3 mL of ethanol, followed by 3 mL of 0.1% ascorbic acid into a 20-mL vial containing 9 mL of phosphate buffer (100 mM, pH 7), giving a 15 mL solution of ^{11}C-CIMBI-5 with a pH of approximately 7. In a total synthesis time of 40–50 min, 1.5–2.5 GBq of ^{11}C-CIMBI-5 was produced, with radiochemical purity greater than 97% and specific radioactivity in the range 64–355 GBq/μmol. The lipophilicity of CIMBI-5 ($cLogD_{7.4}$ [log of calculated distribution coefficient, octanol/buffer pH 7.4]) was calculated using 2 different programs, which were in good agreement (CSLogD [ChemSilico], $cLogD_{7.4}$ = 3.33; Pallas 3.5 [CompuDrug Inc.], $cLogD_{7.4}$ = 3.21).

Ex Vivo Uptake in Rats

Twenty-two Sprague–Dawley rats (mean weight, 295 ± 53 g; Charles River) were included in the study. All animal experiments were performed in accordance with the European Communities Council Resolves of November 24, 1986 (86-609/ECC), and approved by the Danish State Research Inspectorate (journal no. 2007/561-1320). Rats were maintained on a 12-h light–dark cycle, with free access to food and water.

The ex vivo uptake and brain distribution were evaluated as previously described (*17*). Briefly, rats were injected in the tail vein with ^{11}C-CIMBI-5 (3.9 ± 3.5 MBq/kg; specific radioactivity, 30.9 GBq/μmol). The rats were decapitated at 5 (n = 2), 15 (n = 2), 30 (n = 4), 45 (n = 2), and 60 min (n = 4); the brains were quickly removed, placed on ice, and dissected into frontal cortex

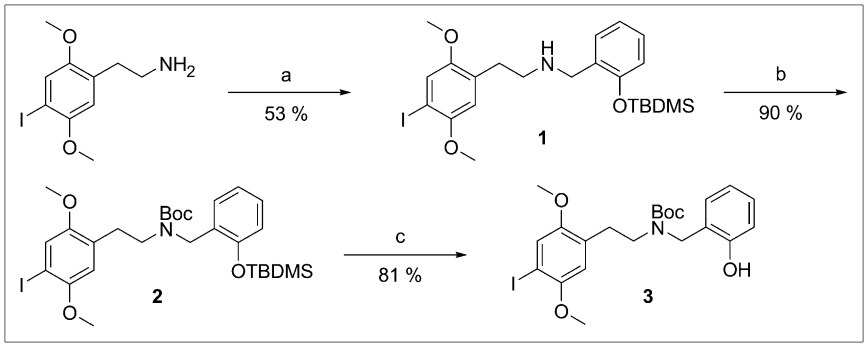

FIGURE 1. Synthesis of labeling precursor for ^{11}C-CIMBI-5 (*3*): (a) 2-(*tert*-butyldimethylsilyloxy)benzaldehyde, $NaBH_4$, MeOH; (b) Boc_2O, THF; and (c) TBAF, NH_4Cl, THF. OTBDMS = t-butyldimethylsiloxy; THF = tetrahydrofuran.

(first 3 mm of the brain) and cerebellum. Blood from the trunk was collected immediately, and plasma was isolated by centrifugation (1,500 rpm, 10 min). All brain tissue samples were collected in tared counting vials and counted for 20 s in a γ-counter (Cobra 5003; Packard Instruments).

For ex vivo blocking studies, rats were divided in vehicle (saline) and ketanserin-treated groups (n = 5–6). Rats were intravenously injected with vehicle or 1 mg/kg of ketanserin (Sigma) 45 min before tracer administration. ^{11}C-CIMBI-5 was injected in the tail vein, and after 30 min, the rats were decapitated. Brain regions and plasma were extracted and counted.

PET in Pigs

Six female Danish Landrace Pigs were used in this study (mean weight, 17.8 ± 1.4 kg). After arrival, animals were housed under standard conditions and were allowed to acclimatize for 1 wk before scanning. On the scanning day, pigs were tranquilized by intramuscular injection of 0.5 mg/kg of midazolam. Anesthesia was induced by 0.1 mL/kg intramuscular injections of Zoletil veterinary mixture (Virbac Animal Health; 125 mg of tiletamine and 125 mg of zolazepam in 8 mL of 5 mg/mL midazolam). After induction, anesthesia was maintained by a 10 mg/kg/h intravenous infusion of propofol (B. Braun Melsugen AG). During anesthesia, animals were endotracheally intubated and ventilated (volume, 250 mL; frequency, 15 per min). Venous access was granted through 2 Venflons (Becton Dickinson) in the peripheral milk veins, and an arterial line for blood sampling measurement was obtained by a catheter in the femoral artery after a minor incision. Vital signs including blood pressure, temperature, and heart rate were monitored throughout the duration of the PET scan. Immediately after scanning, animals were sacrificed by intravenous injection of pentobarbital–lidocaine. All animal procedures were approved by the Danish Council for Animal Ethics (journal no. 2006/561-1155).

PET Protocol

In 5 pigs, ^{11}C-CIMBI-5 was given as intravenous bolus injections, and the pigs were subsequently PET-scanned for 90 min in list mode with a high-resolution research tomography scanner (Siemens AG). Scanning began at the time of injection. After the baseline scan, 3 pigs were maintained in anesthesia and scanned a second time using the same PET protocol. The 5-HT_{2A} receptor antagonist ketanserin tartrate (Sigma) was administered at 30 min before the second scan (3 mg/kg bolus, followed by 1 mg/kg/h infusion for the duration of the scan). For all ^{11}C-CIMBI-5 PET scans, the injected radioactivity was on average 238 MBq (range, 96–418 MBq; n = 9), the specific radioactivity at the time of injection was 75 GBq/μmol (range, 28–133 GBq/μmol; n = 9), the average injected mass was 1.85 μg (range, 0.37–5.49 μg; n = 9), and there were no significant differences in these parameters between the baseline and blocked scans. In 2 pigs, arterial whole-blood samples were taken throughout the entire scan. During the first 15 min after injection, radioactivity in whole blood was continuously measured using an ABSS autosampler (Allogg Technology) counting coincidences in a lead-shielded detector. Concurrently, blood samples were manually drawn at 2.5, 5, 10, 20, 30, 50, 70, and 90 min, and the radioactivity in whole blood and plasma was measured using a well counter (Cobra 5003; Packard Instruments) that was cross-calibrated to the high-resolution research tomography scanner and autosampler. Also, radiolabeled parent compound and metabolites were measured in plasma as in the "HPLC Analysis of Pig Plasma and Pig Brain Tissue" section.

The free fraction of ^{11}C-CIMBI-5 in plasma, f_p, was estimated using an equilibrium dialysis chamber method as previously described (*18*). Briefly, the dialysis was conducted in chambers (Harvard Biosciences) separated by a cellulose membrane with a protein cutoff of 10,000 Da. Small amounts of ^{11}C-CIMBI-5 (~10 MBq) were added to a 5-mL plasma sample from the pig. Plasma (500 μL) was then dialyzed at 37°C against an equal volume of buffer (135 mM NaCl, 3.0 mM KCl, 1.2 mM $CaCl_2$, 1.0 mM $MgCl_2$, and 2.0 mM KH_2PO_4, pH 7.4). Counts per minute in 400 μL of plasma and buffer were determined in a well counter after various dialysis times, and f_p of ^{11}C-CIMBI-5 was calculated as counts per minute in buffer divided by counts per minute in plasma. The samples were taken from the dialysis chambers after equilibrium had been obtained between the 2 chambers.

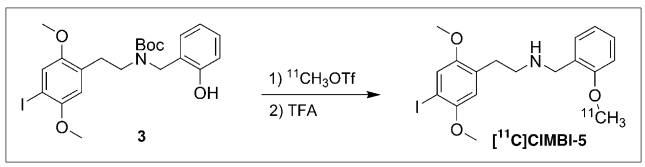

FIGURE 2. Radiochemical synthesis of ^{11}C-CIMBI-5. OTf = triflate; TFA = trifluoroacetic acid.

HPLC Analysis of Pig Plasma and Pig Brain Tissue

Whole-blood samples (10 mL) drawn during PET were centrifuged (3,500 rpm, 4 min), and the plasma was passed through a 0.45-μm filter before HPLC analysis with online radioactivity detection, as previously described (*19*).

Also, the presence of radioactive metabolites of ^{11}C-CIMBI-5 in the pig brain was investigated. Twenty-five minutes after intravenous injection of approximately 500 MBq of ^{11}C-CIMBI-5, the pig was killed by intravenous injection of pentobarbital and

decapitated, and the brain was removed. At the same time, a blood sample was drawn manually. Within 30 min of decapitation, brain tissue was homogenized in 0.1N perchloric acid (Bie and Bentsen) saturated with sodium–ethylenediaminetetraacetic acid (Sigma) for 2 × 30 s using a Polytron homogenizer (Kinematica, Inc.). After centrifugation, the supernatant was neutralized using phosphate buffer, filtered (0.45 μm), and analyzed by HPLC. A plasma sample taken at the time of decapitation was analyzed concurrently.

Quantification of PET Data

Ninety-minute high-resolution research tomography, list-mode PET data were reconstructed into 38 dynamic frames of increasing length (6 × 10, 6 × 20, 4 × 30, 9 × 60, 3 × 120, 6 × 300, and 4 × 600 s). Images consisted of 207 planes of 256 × 256 voxels of 1.22 × 1.22 × 1.22 mm. A summed image of all counts in the 90-min scan was reconstructed for each pig and used for coregistration to a standardized MRI-based statistical atlas of the Danish Landrace pig brain, similar to that previously reported for the Göttingen minipig (*20*), using the program Register as previously described (*18*). The temporal radioactivity in volumes of interest (VOIs), including the cerebellum, cortex (defined in the MRI-based atlas as entire cortical gray matter), hippocampus, lateral and medial thalamus, caudate nucleus, and putamen, was calculated. Radioactivity in all VOIs was calculated as the average of radioactive concentration (Bq/mL) in the left and right sides. Outcome measure in the time–activity curves was calculated as radioactive concentration in VOI (in kBq/mL) normalized to the injected dose corrected for animal weight (in kBq/g), yielding standardized uptake values (g/mL).

In 1 pig in which full arterial input function, including metabolite correction, was measured, we calculated ^{11}C-CIMBI-5 distribution volumes (V_T) for VOIs based on either 1-tissue- or 2-tissue-compartment models (1TC or 2TC, respectively) using plasma corrected for parent compound as the arterial input function (Supplemental Table 1). Cortical nondisplaceable binding potential (BP_{ND}) was calculated as $BP_{ND} = V_T/V_{ND} - 1$ (*21*), assuming that specific 5-HT_{2A} receptor binding in the cerebellum was negligible and that the nondisplaceable volume of distribution (V_{ND}) was equal to the cerebellar V_T (*3*). For all 5 pigs, BP_{ND} was also calculated with the simplified reference tissue model (SRTM) (*22*), both at baseline and in the ketanserin-blocked condition, with the cerebellum as the reference region (Supplemental Table 1). Kinetic modeling was done with PMOD software (version 3.0; PMOD Technologies Inc.). Goodness of fit was evaluated using the Akaike information criterion.

Statistical Analysis

All statistical tests were performed using Prism (version 5.0; GraphPad Software). *P* values below 0.05 were considered statistically significant. Results are expressed in mean ± SD unless otherwise stated.

RESULTS

Chemistry

The labeling precursor was synthesized in 3 steps (Fig. 1): reductive amination with t-butyldimethylsilyl–protected salicylaldehyde, followed by *tert*-butoxycarbonyl (Boc) protection of the secondary amine and removal of the t-butyldimethylsilyl group, which gave the labeling precursor (**3**). Synthesis of the reference compound has been described previously (*13*).

In Vitro Binding Affinity

CIMBI-5 had the highest affinity for the 5-HT_{2A} receptor, in agreement with previous studies (*14*). Between the subtypes of the 5-HT_2 receptors, CIMBI-5 did not show a higher affinity toward 5-HT_{2A} receptors than it did toward 5-HT_{2B} receptors; however, approximately a 3-fold higher affinity of CIMBI-5 for 5-HT_{2A} receptors than for 5-HT_{2C} receptors was found. Against targets other than 5-HT_2 receptors, CIMBI-5 showed at least a 30-fold lower affinity for any other of the investigated receptors than for 5-HT_{2A} receptors (Table 1). In vitro binding assays conducted in our laboratory determined K_i of CIMBI-5 against 2 nM ^{3}H-MDL100907 at 1.5 ± 0.7 nM, thus confirming nanomolar affinity of CIMBI-5 for 5-HT_{2A} receptors.

In Vitro Functional Characterization

The functional properties of CIMBI-5 toward the 5-HT_{2A} receptor were assessed by measuring its effect on phosphoinositide hydrolysis in GF62 cells overexpressing the 5-HT_{2A} receptor. CIMBI-5 was found to be an agonist with an EC_{50} of 1.02 ± 0.17 nM (Supplemental Fig. 1), in agreement with previous reports (*13*). Pretreatment with 1 μM ketanserin completely inhibited CIMBI-5–induced phosphoinositide hydrolysis (data not shown). Furthermore, CIMBI-5 showed 84.6% ± 1.9% of the 5-HT_{2A} activation achieved by 10 μM 5-HT, demonstrating that CIMBI-5 functioned nearly as a full agonist.

Ex Vivo Distribution in Rats

After injection of ^{11}C-CIMBI-5 in awake rats, the time–activity curves measured as standardized uptake values showed highest uptake in the frontal cortex, whereas uptake in the cerebellum (equivalent to nondisplaceable uptake) was lower and paralleled the plasma time–activity curve. The brain uptake peaked in all regions at 15 min after injection and thereafter slowly declined (data not shown).

The specific binding ratio (SBR) in the frontal cortex region of interest, calculated as SBR = (region of interest − cerebellum)/cerebellum, peaked 30 min after injection, reaching a level of 0.77 ± 0.07, after which the SBR slowly declined (Fig. 3A). Thus, 30 min after injection was chosen as a reference time point and used in the blocking experiment with ketanserin. Ketanserin pretreatment reduced the SBR in the frontal cortex to levels not significantly different from zero (0.076 ± 0.12) (Fig. 3B).

In Vivo Distribution and Ketanserin Blockade in Pig Brain

^{11}C-CIMBI-5 showed high cortical uptake in vivo in the pig brain with PET, medium uptake in striatal and thalamic regions, and low uptake in the cerebellum (Fig. 4). Furthermore, the time–activity curves demonstrated a substantial separation between the cortical and cerebellar time–activity curves (Fig. 5A). The time–activity curves peaked at approximately 10 min after injection and thereafter decreased, implying that ^{11}C-CIMBI-5 binding is reversible over the 90-min scan time used in this study.

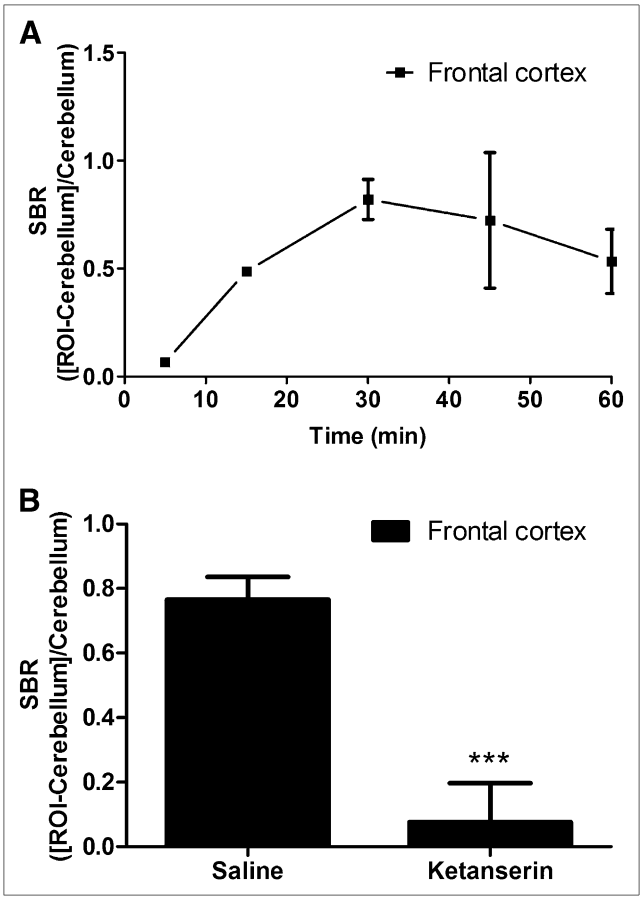

FIGURE 3. Time-dependent ex vivo distribution of ^{11}C-CIMBI-5 and displacement by ketanserin. (A) SBRs in frontal cortex in rats are shown relative to time after injection. (B) After ketanserin pretreatment (1 mg/kg intravenously), SBR in frontal cortex at 30 min after ^{11}C-CIMBI-5 injection is significantly decreased. ***$P < 0.0001$ in Student t test of ketanserin vs. saline. ROI = region of interest.

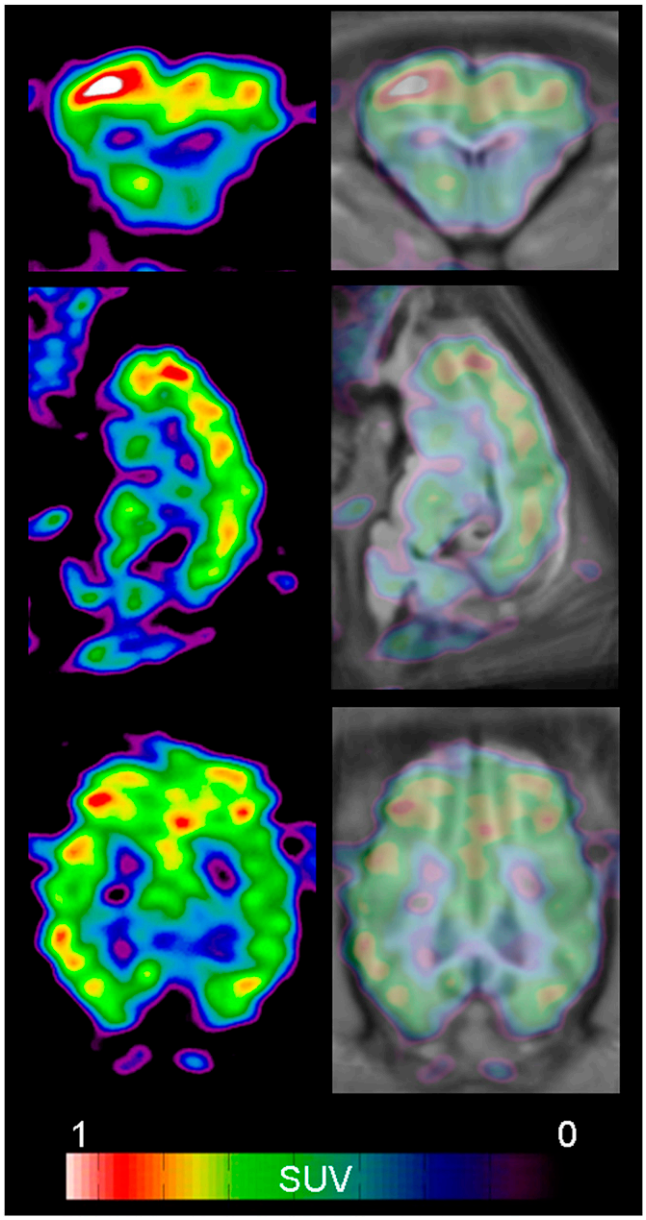

FIGURE 4. Representative coronal (top), sagittal (middle), and horizontal (bottom) PET images summed from 0 to 90 min of scanning showing distribution of ^{11}C-CIMBI-5 in pig brain. Left column shows PET images after 3 × 3 × 3 mm gaussian filtering. Right column shows same PET images aligned and overlaid on a standardized MRI-based atlas of the pig brain after coregistration. SUV = standardized uptake value.

After ketanserin treatment, the concentration of ^{11}C-CIMBI-5 in the cortex was reduced almost completely to cerebellar levels (Fig. 5A). The cerebellar time–activity curve was unaltered by ketanserin administration (Fig. 5A).

Kinetic Modeling

With the SRTM, baseline cortical BP_{ND} of ^{11}C-CIMBI-5 was 0.46 ± 0.11 (n = 5). After the ketanserin bolus and infusion, the cortical BP_{ND} was significantly decreased by 75% (mean blocked BP_{ND}, 0.11 ± 0.06; n = 3). For the fitted SRTM, no significant difference in goodness of fit was found between baseline and blocked condition (Supplemental Table 1). In 1 pig in which full metabolite-corrected arterial input was measured, V_T was calculated from 1TC and 2TC models. Ratios between V_T in the cortex and cerebellum were 1.57 and 1.61, corresponding to a BP_{ND} of 0.57 and 0.61 with the 1TC and 2TC model, respectively. After ketanserin blockade, cortical ^{11}C-CIMBI-5 BP_{ND} was reduced to 0.13 and 0.11 in the 1TC and 2TC, respectively (Supplemental Table 1).

Radiolabeled Metabolites

In the radio-HPLC analysis, a lipophilic radioactive metabolite accounting for up to 20% of the total plasma radioactivity was found, and it maintained stable plasma levels after 20 min and throughout the scan (Fig. 6). The HPLC retention time of ^{11}C-CIMBI-5 and its metabolite in the HPLC column suggest that the metabolite is slightly less lipophilic than ^{11}C-CIMBI-5 itself (Fig. 7). However, this metabolite was found only in negligible amounts in homogenized pig brain tissue, compared with plasma from the same animal (Fig. 7).

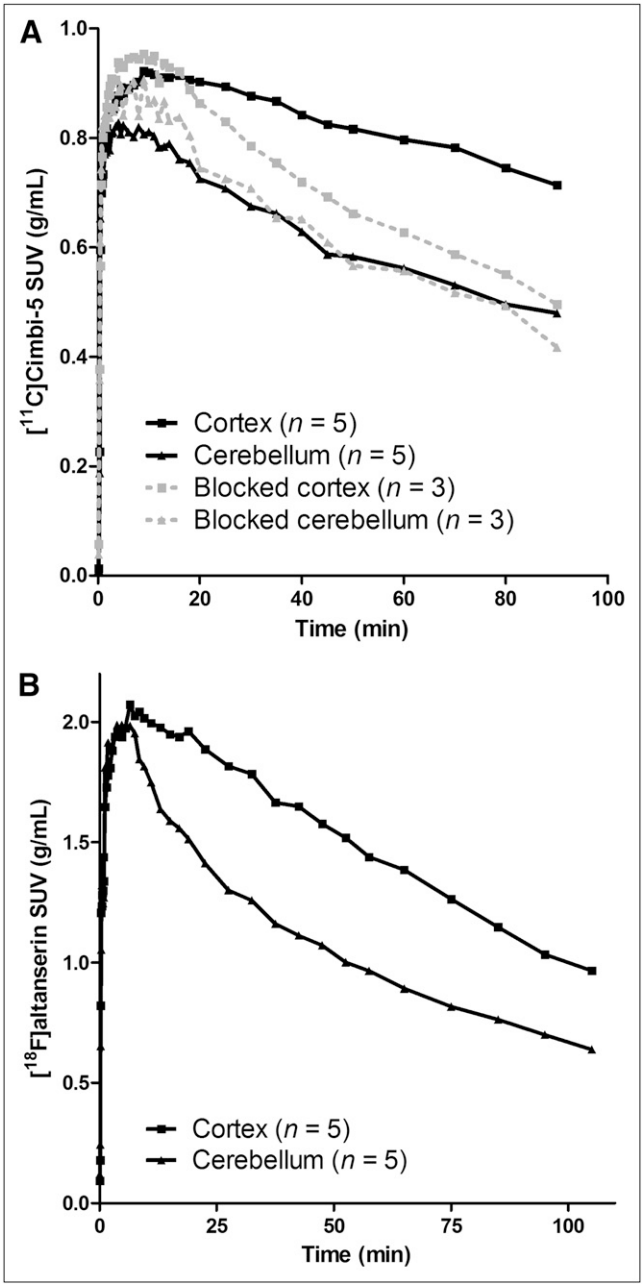

FIGURE 5. Time–activity curves of 5-HT_{2A} agonist and antagonist PET tracers in pig brain. (A) ^{11}C-CIMBI-5 time–activity curves in Danish Landrace pig brain at baseline (black solid line) or after intravenous ketanserin (3 mg/kg bolus, 1 mg/kg/h infusion) blockade (gray dotted line). (B) ^{18}F-altanserin time–activity curves in minipigs. Mean standardized uptake values normalized to injected dose per body weight are shown. SUV = standardized uptake value.

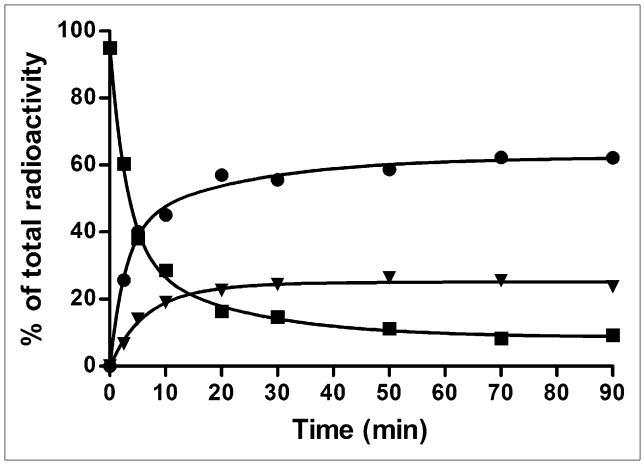

FIGURE 6. HPLC analysis of radioactive metabolites in pig plasma after intravenous injection of ^{11}C-CIMBI-5. ■ = parent compound ^{11}C-CIMBI-5; ▼ = lipophilic metabolite; ● = polar metabolites.

The free fraction of ^{11}C-CIMBI-5 in pig plasma at 37°C was 1.4% ± 0.3% using a dialysis chamber method, in which equilibrium between chambers was reached after 60 min.

DISCUSSION

In the current study, we report the in vitro, ex vivo, and in vivo validation of ^{11}C-CIMBI-5, a novel 5-HT_{2A} receptor agonist PET tracer. To our knowledge, this is the first agonist 5-HT_{2A} receptor PET tracer that has been developed. In vitro assays performed at our laboratory, along with assays performed through the PDSP screening program, confirmed the nanomolar affinity of CIMBI-5 for the 5-HT_{2A} receptor as previously reported (*13,14*). In the current study, the K_i for CIMBI-5 against ^{3}H-MDL100907 was 1.5 ± 0.7 nM, in agreement with the PDSP value of 2.2 nM for K_i of CIMBI-5 against ^{3}H-ketanserin. The somewhat lower value (K_i = 0.15 nM against ^{3}H-ketanserin) previously reported (*13*) may have been because that assay was performed at 25° C, whereas the values reported here were obtained at 37°C. We also confirmed that CIMBI-5 has agonistic properties at the 5-HT_{2A} receptor, with an EC_{50} value of 1.02 ± 0.17 nM, in agreement with previous reports (*13*). In addition, we showed that CIMBI-5 is nearly a full agonist, with 85% of the 5-HT_{2A} activation, compared with 5-HT itself. The data on binding and receptor activation, taken together with the PDSP screening for CIMBI-5 (Table 1), show that CIMBI-5 is a high-affinity agonist for 5-HT_{2A} receptors. CIMBI-5 had an affinity similar to that of the 5-HT_{2A} and the 5-HT_{2B} receptors and a 3-fold lower affinity to 5-HT_{2C} receptor. The eventual presence and distribution of 5-HT_{2B} receptors in the brain is still questionable, and specific 5-HT_{2B} receptor binding in the brain has to our knowledge not yet been demonstrated. For 5-HT_{2C} receptors, density of this subtype of receptors in cortical areas, compared with density of 5-HT_{2A} receptors, is negligible (*23,24*). Therefore, the cortical ^{11}C-CIMBI-5 binding signal stems from its 5-HT_{2A} receptor binding.

^{11}C-CIMBI-5 uptake and distribution in the rat brain after ex vivo dissection were similar to those in previous rat studies with ^{18}F-altanserin (*25*), showing high uptake in the frontal cortex and no displaceable binding in the cerebellum. Also, the specific uptake in the frontal cortex of the rat brain was blocked by ketanserin pretreatment, indicating that ^{11}C-CIMBI-5 binding is selective for the 5-HT_{2A} receptor. Similarly, ^{11}C-CIMBI-5 distributed in the pig

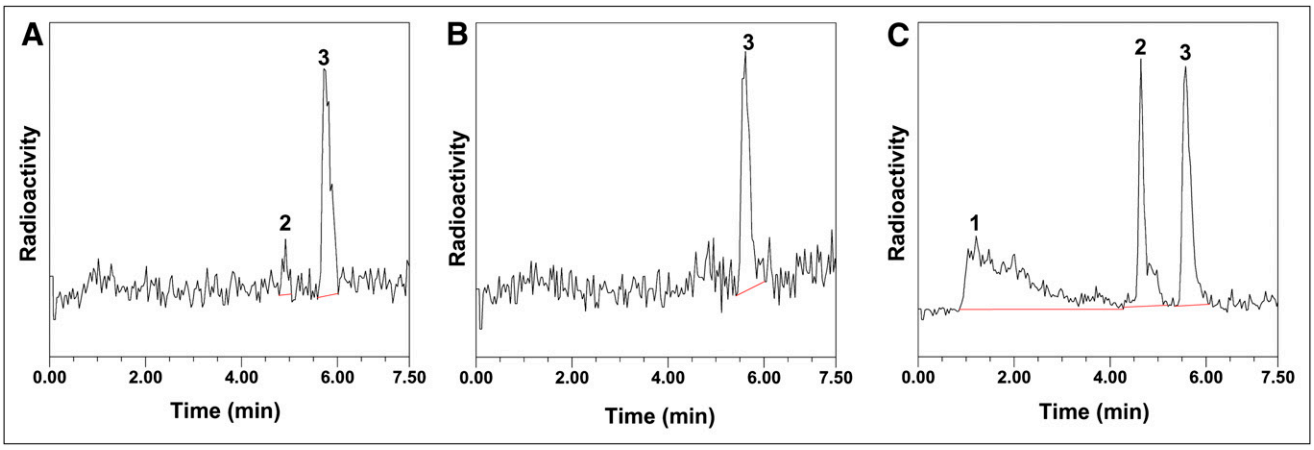

FIGURE 7. HPLC analysis of brain extracts and plasma at 25 min after injection of ^{11}C-CIMBI-5: frontal cortex (A), cerebellum (B), and plasma (C). Peaks: 1 = polar metabolites, 2 = lipophilic metabolites, and 3 = parent compound.

brain in a pattern resembling the 5-HT_{2A} receptor distribution as measured with 5-HT_{2A} receptor antagonist PET tracers in pigs (*25*) and in humans (*5,26*), with high cortical uptake and low cerebellar uptake. Further, the 5-HT_{2A} selectivity of in vivo cortical ^{11}C-CIMBI-5 binding in the pig was confirmed in the blocking study in which cortical ^{11}C-CIMBI-5 binding was decreased by a ketanserin bolus and infusion, whereas the cerebellar uptake was unaffected.

BP_{ND} for ^{11}C-CIMBI-5 with the cerebellum as a reference region was calculated using compartmental models, reference tissue approaches, and noninvasive Logan methods (Supplemental Table 1). For 5-HT_{2A} receptor antagonist PET tracers, such as ^{18}F-altanserin, the cerebellum is generally regarded as a valid reference region (*3*). Also, because negligible amounts of 5-HT_{2A} receptors are present in the cerebellum, compared with cortical areas, the preferential binding of a 5-HT_{2A} receptor PET ligand, as measured, for example, by the SRTM BP_{ND}, is indicative of the target-to-background ratio of 5-HT_{2A} PET ligands. At baseline, ^{11}C-CIMBI-5 showed an average SRTM BP_{ND} of 0.46. Given that an agonist PET tracer, compared with the antagonist, would bind only a high-affinity subpopulation of 5-HT_{2A} receptors, the maximum number of binding sites for such an agonist tracer would be lower than the antagonist, and—given that the radioligand affinities are comparable—it is anticipated that a lower BP_{ND} for an agonist tracer would be found. When compared with human data from 5-HT_{2A} receptor antagonist PET tracers (*5,26*), the cortical binding potential of ^{11}C-CIMBI-5 was indeed lower, but further studies are required to explore whether the somewhat low binding potential measured in pigs will translate to humans.

To compare the time–activity curves for ^{11}C-CIMBI-5 to a known 5-HT_{2A} antagonist PET tracer in the same animal species, we compared it to ^{18}F-altanserin pig data obtained from our laboratory (*25*). ^{11}C-CIMBI-5 and ^{18}F-altanserin in pigs showed similar cortex-to-cerebellum uptake and equal SRTM BP_{ND}, 0.46 ± 0.11 and 0.47 ± 0.10, respectively. Thus, in the pig brain ^{11}C-CIMBI-5 and ^{18}F-altanserin have similar target-to-background binding ratios, and ^{11}C-CIMBI-5 therefore holds promise for clinical use.

After injection of ^{11}C-CIMBI-5, a radiolabeled metabolite only slightly less lipophilic than ^{11}C-CIMBI-5 appeared in the pig plasma. On the basis of previous studies describing the metabolism of the 5-HT_{2A} receptor agonist compound 1-(2,5-dimethoxy-4-iodophenyl)-2-aminopropane (*27*) in rats, we speculated that this metabolite is the result of *O*-demethylation at a methoxy group in the iododimethoxyphenyl moiety of the tracer. Lipophilic radiolabeled metabolites impose a problem if they cross the blood–brain barrier because their presence will contribute to nonspecific binding. This has been observed for other antagonistic PET tracers in the serotonin system (*3*). Our brain homogenate experiments suggested that the lipophilic metabolite does not enter the pig brain, at least not to any large extent, and consequently the radiolabeled metabolite does not contribute to the nonspecific binding of ^{11}C-CIMBI-5.

Taken together, the results indicate that ^{11}C-CIMBI-5 is a promising tracer for visualization and quantification of high-affinity 5-HT_{2A} receptor agonist binding sites using PET. More specifically, studies of ^{11}C-CIMBI-5 could reveal differences in the number of binding sites measured with an agonist versus antagonist tracer, thus giving insights to whether high- and low-affinity states of 5-HT_{2A} receptors coexist in vivo as is described for the dopamine system (*28*). Optimally, a larger cortical BP_{ND} and higher brain uptake of the PET tracer is preferred. Also, the time–activity curves of ^{11}C-CIMBI-5 suggested relatively slow kinetics, which potentially would be a more pronounced phenomenon in primates and humans complicating quantification. Therefore, it may be worthwhile to pursue development of ^{11}C-CIMBI-5 analogs with modified chemical structures to improve these PET tracer properties.

CONCLUSION

The novel high-affinity 5-HT_{2A} receptor agonist PET tracer ^{11}C-CIMBI-5 distributes in the brain in a pattern compatible with the known 5-HT_{2A} receptor distribution,

and its binding can be blocked by ketanserin treatment. ^{11}C-CIMBI-5 is a promising PET tracer for in vivo imaging and quantification of high-affinity-state 5-HT$_{2A}$ receptors in the human brain.

ACKNOWLEDGMENTS

The study was financially supported by the Lundbeck Foundation, the Faculty of Health Sciences and the Faculty of Pharmaceutical Sciences at the University of Copenhagen, and by the EU 6th Framework program DiMI (LSHB-CT-2005-512146). K_i determinations were generously provided by the NIMH PDSP. A reference sample of CIMBI-5 was kindly provided by David Nichols, Purdue University.

REFERENCES

1. Gonzalez-Maeso J, Weisstaub NV, Zhou M, et al. Hallucinogens recruit specific cortical 5-HT$_{2A}$ receptor-mediated signaling pathways to affect behavior. *Neuron.* 2007;53:439–452.
2. Kim SW, Shin IS, Kim JM, et al. The 5-HT2 receptor profiles of antipsychotics in the pathogenesis of obsessive-compulsive symptoms in schizophrenia. *Clin Neuropharmacol.* 2009;32:224–226.
3. Pinborg LH, Adams KH, Svarer C, et al. Quantification of 5-HT2A receptors in the human brain using [^{18}F]altanserin-PET and the bolus/infusion approach. *J Cereb Blood Flow Metab.* 2003;23:985–996.
4. Soares JC, van Dyck CH, Tan P, et al. Reproducibility of in vivo brain measures of 5-HT2A receptors with PET and [^{18}F]deuteroaltanserin. *Psychiatry Res.* 2001;106:81–93.
5. Ito H, Nyberg S, Halldin C, Lundkvist C, Farde L. PET imaging of central 5-HT2A receptors with carbon-11-MDL 100,907. *J Nucl Med.* 1998;39:208–214.
6. Fitzgerald LW, Conklin DS, Krause CM, et al. High-affinity agonist binding correlates with efficacy (intrinsic activity) at the human serotonin 5-HT2A and 5-HT2C receptors: evidence favoring the ternary complex and two-state models of agonist action. *J Neurochem.* 1999;72:2127–2134.
7. Song J, Hanniford D, Doucette C, et al. Development of homogeneous high-affinity agonist binding assays for 5-HT2 receptor subtypes. *Assay Drug Dev Technol.* 2005;3:649–659.
8. Cornea-Hebert V, Watkins KC, Roth BL, et al. Similar ultrastructural distribution of the 5-HT$_{2A}$ serotonin receptor and microtubule-associated protein MAP1A in cortical dendrites of adult rat. *Neuroscience.* 2002;113:23–35.
9. Peddie CJ, Davies HA, Colyer FM, Stewart MG, Rodriguez JJ. Colocalisation of serotonin2A receptors with the glutamate receptor subunits NR1 and GluR2 in the dentate gyrus: an ultrastructural study of a modulatory role. *Exp Neurol.* 2008;211:561–573.
10. Cumming P, Wong DF, Gillings N, Hilton J, Scheffel U, Gjedde A. Specific binding of [^{11}C]raclopride and *N*-[^{3}H]propyl-norapomorphine to dopamine receptors in living mouse striatum: occupancy by endogenous dopamine and guanosine triphosphate-free G protein. *J Cereb Blood Flow Metab.* 2002;22:596–604.
11. Narendran R, Hwang DR, Slifstein M, et al. In vivo vulnerability to competition by endogenous dopamine: comparison of the D2 receptor agonist radiotracer (−)-*N*-[^{11}C]propyl-norapomorphine ([^{11}C]NPA) with the D2 receptor antagonist radiotracer [^{11}C]-raclopride. *Synapse.* 2004;52:188–208.
12. Pinborg LH, Adams KH, Yndgaard S, et al. [^{18}F]altanserin binding to human 5HT2A receptors is unaltered after citalopram and pindolol challenge. *J Cereb Blood Flow Metab.* 2004;24:1037–1045.
13. Braden MR, Parrish JC, Naylor JC, Nichols DE. Molecular interaction of serotonin 5-HT2A receptor residues Phe339(6.51) and Phe340(6.52) with superpotent *N*-benzyl phenethylamine agonists. *Mol Pharmacol.* 2006;70:1956–1964.
14. Nichols DE, Frescas SP, Chemel BR, Rehder KS, Zhong D, Lewin AH. High specific activity tritium-labeled *N*-(2-methoxybenzyl)-2,5-dimethoxy-4-iodophenethylamine (INBMeO): a high-affinity 5-HT2A receptor-selective agonist radioligand. *Bioorg Med Chem.* 2008;16:6116–6123.
15. Herth MM, Kramer V, Piel M, et al. Synthesis and in vitro affinities of various MDL 100907 derivatives as potential ^{18}F-radioligands for 5-HT2A receptor imaging with PET. *Bioorg Med Chem.* 2009;17:2989–3002.
16. Kramer V, Herth MM, Santini MA, Palner M, Knudsen GM, Rosch F. Structural combination of established 5-HT receptor ligands: new aspects of the binding mode. *Chem Biol Drug Des.* 2010;76:361–366.
17. Palner M, McCormick P, Gillings N, Begtrup M, Wilson AA, Knudsen GM. Radiosynthesis and ex vivo evaluation of (*R*)-(−)-2-chloro-*N*-[1-^{11}C-propyl]n-propylnorapomorphine. *Nucl Med Biol.* 2010;37:35–40.
18. Kornum BR, Lind NM, Gillings N, Marner L, Andersen F, Knudsen GM. Evaluation of the novel 5-HT4 receptor PET ligand [^{11}C]SB207145 in the Gottingen minipig. *J Cereb Blood Flow Metab.* 2009;29:186–196.
19. Gillings N. A restricted access material for rapid analysis of [^{11}C]-labeled radiopharmaceuticals and their metabolites in plasma. *Nucl Med Biol.* 2009;36:961–965.
20. Watanabe H, Andersen F, Simonsen CZ, Evans SM, Gjedde A, Cumming P. MR-based statistical atlas of the Gottingen minipig brain. *Neuroimage.* 2001;14:1089–1096.
21. Innis RB, Cunningham VJ, Delforge J, et al. Consensus nomenclature for in vivo imaging of reversibly binding radioligands. *J Cereb Blood Flow Metab.* 2007;27:1533–1539.
22. Lammertsma AA, Hume SP. Simplified reference tissue model for PET receptor studies. *Neuroimage.* 1996;4:153–158.
23. Kristiansen H, Elfving B, Plenge P, Pinborg LH, Gillings N, Knudsen GM. Binding characteristics of the 5-HT2A receptor antagonists altanserin and MDL 100907. *Synapse.* 2005;58:249–257.
24. Marazziti D, Rossi A, Giannaccini G, et al. Distribution and characterization of [^{3}H]mesulergine binding in human brain postmortem. *Eur Neuropsychopharmacol.* 1999;10:21–26.
25. Syvanen S, Lindhe O, Palner M, et al. Species differences in blood-brain barrier transport of three positron emission tomography radioligands with emphasis on P-glycoprotein transport. *Drug Metab Dispos.* 2009;37:635–643.
26. Adams KH, Pinborg LH, Svarer C, et al. A database of [^{18}F]-altanserin binding to 5-HT$_{2A}$ receptors in normal volunteers: normative data and relationship to physiological and demographic variables. *Neuroimage.* 2004;21:1105–1113.
27. Ewald AH, Fritschi G, Maurer HH. Metabolism and toxicological detection of the designer drug 4-iodo-2,5-dimethoxy-amphetamine (DOI) in rat urine using gas chromatography-mass spectrometry. *J Chromatogr B Analyt Technol Biomed Life Sci.* 2007;857:170–174.
28. Laruelle M. Imaging synaptic neurotransmission with in vivo binding competition techniques: a critical review. *J Cereb Blood Flow Metab.* 2000;20:423–451.

The Journal of NUCLEAR MEDICINE

Radiosynthesis and Evaluation of ^{11}C-CIMBI-5 as a 5-HT$_{2A}$ Receptor Agonist Radioligand for PET

Anders Ettrup, Mikael Palner, Nic Gillings, Martin A. Santini, Martin Hansen, Birgitte R. Kornum, Lars K. Rasmussen, Kjell Någren, Jacob Madsen, Mikael Begtrup and Gitte M. Knudsen

J Nucl Med. 2010;51:1763-1770.
Published online: October 18, 2010.
Doi: 10.2967/jnumed.109.074021

The Journal of Nuclear Medicine is published monthly.
SNMMI | Society of Nuclear Medicine and Molecular Imaging
1850 Samuel Morse Drive, Reston, VA 20190.
(Print ISSN: 0161-5505, Online ISSN: 2159-662X)

SNMMI SOCIETY OF NUCLEAR MEDICINE AND MOLECULAR IMAGING